



Montréal, Québec
May 29 to June 1, 2013 / 29 mai au 1 juin 2013

Preliminary Investigation on Punching-Shear Strength of Flat Slabs with FRP Flexural and Shear Reinforcement

Mohamed Hassan, Ehab Ahmed, and Brahim Benmokrane
Department of Civil Engineering, University of Sherbrooke, Sherbrooke, Quebec, Canada

Abstract: This preliminary study investigates the punching-shear behaviour of flat slabs reinforced in flexure and shear with FRP reinforcement. Three full-scale interior slab-column connections were constructed and tested under concentric loading until failure. The three specimens were reinforced in flexure with glass fiber-reinforced polymer (GFRP) bars. However, two of them were reinforced in shear with carbon and glass FRP spiral stirrups and the third one was kept without shear reinforcement to serve as reference for comparison. The slabs measured 2500 mm × 2500 mm × 350 mm and a square column of 300 mm × 300 mm. The tests were conducted to evaluate the efficiency and contribution of FRP spiral stirrups (shear reinforcement) to the punching-shear capacity. The test results revealed that using FRP shear reinforcement in form of spiral stirrups in the GFRP-reinforced concrete (GFRP-RC) flat slabs was an effective way to increase the punching-shear capacity. The specimens showed increase in the punching-shear strengths of 37% and 16% for the CFRP and GFRP spiral stirrups, respectively.

1 Introduction

Punching shear capacity of flat slabs can be increased by providing drop panels, column capitals, structural steel shear heads, or stirrups. Using punching-shear reinforcement, however, is not only increases the capacity, but also increases the ductility of the slab-column connection comparative to drop panels and column heads. Furthermore, the shear reinforcement is a preferred solution when the slab thickness is not allowed to increase which, in turn, reduces the slab self-weight and total height of the structure.

The use of fiber-reinforced polymer (FRP) reinforcing bars as main reinforcement for concrete structures in severe environments is becoming a widely accepted solution to overcome the problem of steel corrosion and the related deteriorations. However, few studies were conducted to address the FRP shear reinforcement for flat slabs and quantify the contribution of FRP shear reinforcement to the punching-shear strength. El-Ghandour et al. (2003) tested three specimens reinforced with FRP bars in flexural and carbon FRP shearbands as shear reinforcement. The test results indicated that the shear reinforcement increases the punching-shear capacity by an average ratio of 15.9%. It also plays a role in delaying the bond slip and preventing the punching-shear failure at lower load levels. In addition, larger deformability was demonstrated in the slabs with shear reinforcement compared to slabs without shear reinforcement. Zaghoul (2007) tested four specimens reinforced with FRP grids in flexure and specially manufactured carbon FRP shear rail in shear. The test results showed that the shear reinforcement increased the punching-shear capacity of interior slab-column connection by 24.6% and 30.4%, when the first leg of the shear reinforcement was located at $0.5d$ and $0.85d$, respectively. This increase in punching-shear capacity is comparable to the increase that can be achieved when using steel-headed studs. More

investigation, however, is required to understand the structural behavior of the FRP-reinforced concrete (FRP-RC) flat slabs with FRP shear reinforcement.

An extensive research project has been conducted at the University of Sherbrooke to investigate the behavior of GFRP-RC flat slabs with and without FRP shear reinforcement. The first and second phases of this project for flat slabs without shear reinforcement were completed and their findings contributed to field implementation of GFRP bars in two parking garages in Quebec City which are Hotel de Ville in 2010 and La Chancelière in 2011 (Benmokrane et al. 2012). This paper presents preliminary results of the third phase of this research project which investigates the punching-shear behavior of GFRP-RC two-way flat slabs reinforced with carbon and glass FRP spiral stirrups as shear reinforcement.

2 Experimental Work

2.1 Test specimens

This paper presents experimental results of three full-scale GFRP-RC flat slabs constructed and tested to failure under monotonically concentric loading. The test specimens measured 2500 mm × 2500 mm with thickness of 350 mm and a square column of 300 mm × 300 mm extending 300 mm beyond the top and bottom surfaces of the slabs. Two specimens were reinforced with GFRP and CFRP spiral stirrups while the third one was the reference one without shear reinforcement. The slabs were provided with relatively high flexural reinforcement ratio (1.60%) to ensure punching-shear failure of the three slabs rather than flexural failure. Table 1 presents the characteristics for each specimen. Both of the used carbon and glass FRP spiral stirrups were of size No. 13 and were distributed along central axes of symmetry in X and Y directions with a spacing of $d/4=70$ mm, where d is the effective slab depth (= 280 mm). The clear concrete cover was kept constant at 45 mm. Figure 1 shows the details of test specimens and the flexural and shear reinforcement configurations.

The test specimens were labeled with a letter denoting the flexural reinforcement type (G for GFRP bars) with a subscript indicating the reinforcement ratio, followed by the slab thickness in millimeters (350 mm) and ended by the stirrups configurations (shear reinforcement type, shape, and spacing), if any. For example, the specimen $G_{(1.6)}350\text{-GSS}(d/4)$ was reinforced with GFRP bars with a reinforcement ratio of 1.6% in each direction, a slab thickness of 350 mm, and GFRP shear reinforcement spiral stirrups with spaced at distance $d/4$, where d is the effective slab depth (= 280 mm).

Table 1: Details of test specimens

Prototype	Slab thick., mm	Reinf.	ρ_f , %	ρ_{fv}^a , %	$\rho_{fv}E_{fv}^b$, GPa	f'_c , MPa	f_t , MPa	Shear Reinforcement		
								Type	Diam.	s, mm
$G_{(1.6)}350$		22 No. 25	1.61	-	-	38.2	3.3	-	-	-
$G_{(1.6)}350\text{-GSS}(d/4)$	350	22 No. 25	1.61	0.64	28	40.2	3.3	GFRP	No.13	70
$G_{(1.6)}350\text{-CSS}(d/4)$		22 No. 25	1.61	0.64	79	38.2	3.3	CFRP	No.13	70

^a ρ_{fv} was calculated at a perimeter at $d/2$ from the edge of the column support ($n_s \cdot A_{fv} / S_{fv} \cdot b_{c0.5d}$).

^b ($\rho_{fv} E$) is the shear reinforcement index.

2.2 Material properties

Sand-coated GFRP bars No. 25, designated according to the CSA S807 (2010), were used as flexural reinforcement of the test specimens. Sand-coated CFRP and GFRP spiral stirrups (No. 13) were used as shear reinforcement in the two test specimens with shear reinforcement. Figure 1 shows the reinforcement configurations. The tensile properties of the GFRP bars and the straight portions of CFRP and GFRP stirrups were determined by testing five representative bars in accordance with ASTM D7205 (2011). The tensile strength and tensile modulus of elasticity of the GFRP bars were 1065 ± 22 MPa, and 56.7 ± 0.3 GPa, respectively. The tensile strengths and tensile moduli of elasticity of the straight portions of GFRP and CFRP stirrups, directly cut from the GFRP and CFRP stirrups, were 1004 ± 19 , and 1564 ± 30 MPa and 44.6 ± 0.4 GPa, and 124.4 ± 0.7 GPa, respectively. Tables 2 and 3 provide the mechanical properties of the GFRP bars and the straight portions of the GFRP and CFRP stirrups, respectively.

The specimens were cast using a ready-mixed, normal-weight concrete with a 28-day target concrete compressive strength of 35 MPa and 5 to 8% of entrained air. The concrete compressive (f'_c) and tensile strength (f_t) were determined on the day of testing using three concrete cylinders measuring 150 mm x 300 mm for each test (compression and splitting tests). The average concrete compressive strength was 39 MPa while the average tensile strength was 3.3 MPa. Table 1 provides the concrete properties of the test specimens.

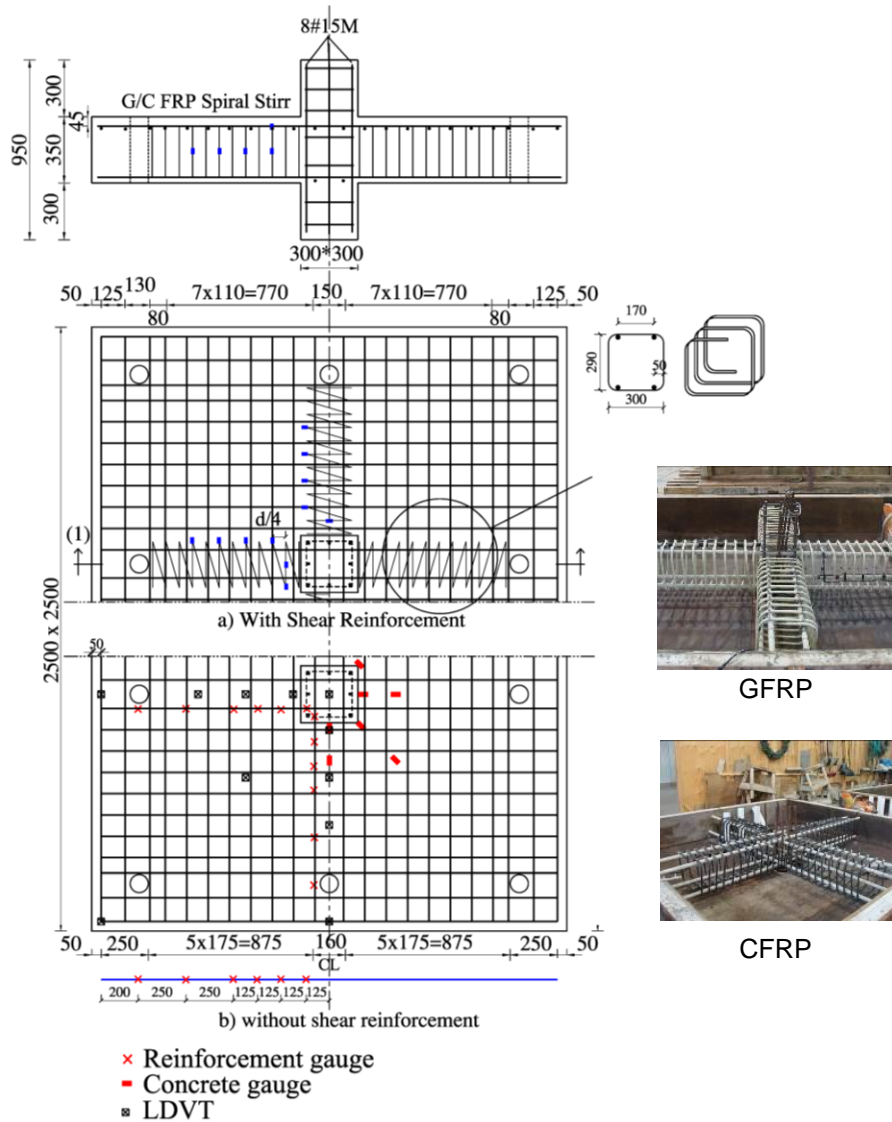


Figure 1: Details of test specimens: geometry, reinforcement configuration, and instrumentations

Table 2: Mechanical properties of GFRP flexural reinforcement

Bar size	Area, mm ²	Tensile modulus, E_f , GPa	Ultimate tensile strength, f_{tu} , MPa	Characteristic tensile strength, f_{tu}^* , MPa ^a	Ultimate elongation, %
No. 25	510	56.7±0.3	1065±22	999	1.88±0.04

^a Characteristic tensile strength = Average value – 3 x standard deviation.

Table 3: Mechanical properties of the FRP shear reinforcement (straight portions)

Stirrup type	Bar size	d_b , mm	r_b , mm	Tensile modulus, E_{fv} , GPa	Ultimate tensile strength, f_{fv} , MPa	Ultimate elongation, (Straight) %
GFRP	No. 13	12.7	50	44.6±0.4	1004±19	2.25±0.06
CFRP	No. 13	12.7	50	124.4±0.7	1564±30	1.26±0.03

2.3 Instrumentations and test setup

Each slab was provided with two instrumented bars in the top reinforcing mat (tension side) with six electrical strain gauges attached to each bar. While six electrical strain gauges were glued in the straight, top bend, and bottom portions of the stirrups in each direction. Eight concrete electrical strain gauges were glued to the slab's bottom surface (compression side) before testing. Moreover, the eight steel anchors supporting the specimen were instrumented with electrical strain gauges to verify loading symmetry during the test. Eleven linear variable differential transducers (LVDTs) were installed to measure the deflection of the slab at the desired locations. The strain gauges and LVDTs were connected to a data-acquisition system to record the readings during the test. Figure 1 shows the instrumentation details. During the test, crack propagation was marked and the corresponding loads were recorded.

The specimens were tested under monotonic loading until failure. The load was applied at a load-controlled rate of 5 kN/min. The load was applied using two 1500 kN hydraulic jacks, until the punching-shear failure occurred. The two hydraulic jacks were connected to the same pump and calibrated to work simultaneously. The test specimens were held against the laboratory's rigid floor using a rigid steel frame 100 mm in width supported by eight steel anchors, each measuring 38 mm in diameter. The tested specimens had a clear span of 1900 mm. Before placing the steel frame, a 15 mm thick layer of cement mortar was placed on the concrete surface at the location of the steel frame. Thereafter, to prevent local failure and to distribute the load uniformly, 10 mm thick neoprene sheets were used over the loading plate and between the supporting frame and the slab, respectively. Figure 2 provides the details of the test setup.

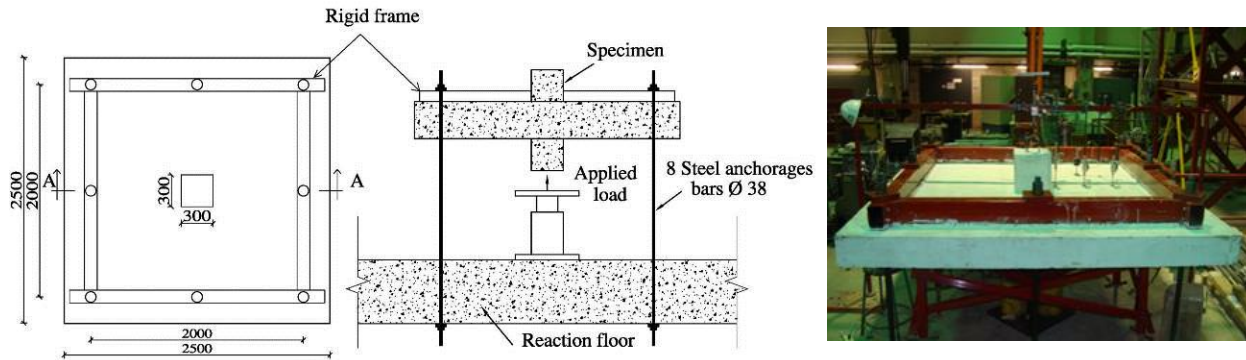


Figure 2: Test setup

3 Test Results and Discussions

3.1 Punching-shear capacity

Table 4 provides the ultimate punching-shear capacities and the corresponding normalized punching-shear stresses calculated at $0.5d$ from the column face. It should be noted that the reported loads include the self-weight of the specimens. The punching-shear stresses at failure were normalized to the cubic root of the concrete strength to account for the variation in the concrete strengths. Table 4 shows that the FRP spiral stirrups increases the ultimate punching-shear capacity of the tested slabs. Compared to the reference slab ($G_{(1.6)350}$ -without shear reinforcement), specimens $G_{(1.6)350}$ -GSS($d/4$), and $G_{(1.6)350}$ -CSS($d/4$) showed increases in the normalized punching-shear stress at failure by 16% and 37%,

respectively. The increase was higher in case of CFRP spiral stirrups than that of GFRP spiral stirrups due to the higher modulus of elasticity of CFRP compared to that of the GFRP.

3.2 Crack patterns and failure mode

The test specimens (with and without shear reinforcement) showed similar crack propagation in the tension side of the slab (top surface). The flexural cracks started from at column corner towards to the slab edges along the central axes of symmetry (X and Y directions). At higher loading (at about 55% of the ultimate load), tangential cracks were developed outside the column location connecting the radial cracks together. The final failure was developed by the column punching through the slab. The test specimens at failure are shown in Figure 3. The test specimen without shear reinforcement showed a sudden and brittle punching-shear failure. However, the specimens with shear reinforcement showed more cracks and exhibited larger post-peak deflection which provides some deformability to the specimens before failure. The punching-shear cone at failure was considerably larger in the specimens with shear reinforcement.

The slab cross-sections shown in Figure 3 indicated that the specimen without shear reinforcement exhibited a main diagonal shear crack starting from the column face to the tension side of the slab followed by a horizontal splitting crack at the level of the flexural reinforcement. The test specimens reinforced with FRP spiral stirrups, however, exhibited many inclined shear cracks starting from the column face and ending by a horizontal splitting crack at the level of the flexural reinforcement. The distance defining the failure surface area (X_{cone}) (the observed distance from column face until the location of the failure surface) was measured at different locations for each specimen and the average values were calculated and reported in Table 4 (multiplications of d).

Table 4: Summary of test results

Prototype	V_{cr} , kN	Δ_{cr} mm	V_u , kN	$v_u^3 \sqrt{f_c'}$	X_{cone}	ϵ_{fmax} , ($\mu\epsilon$)	ϵ_{cmax} , ($\mu\epsilon$)
G _(1.6) 350	583	1.77	1492	0.68	1.7d	3199	-2385
G _(1.6) 350-GSS(d/4)	631	3.23	1761	0.79	2.0d	4265	-1770
G _(1.6) 350-CSS(d/4)	619	3.03	2024	0.93	2.5d	6801	-3740

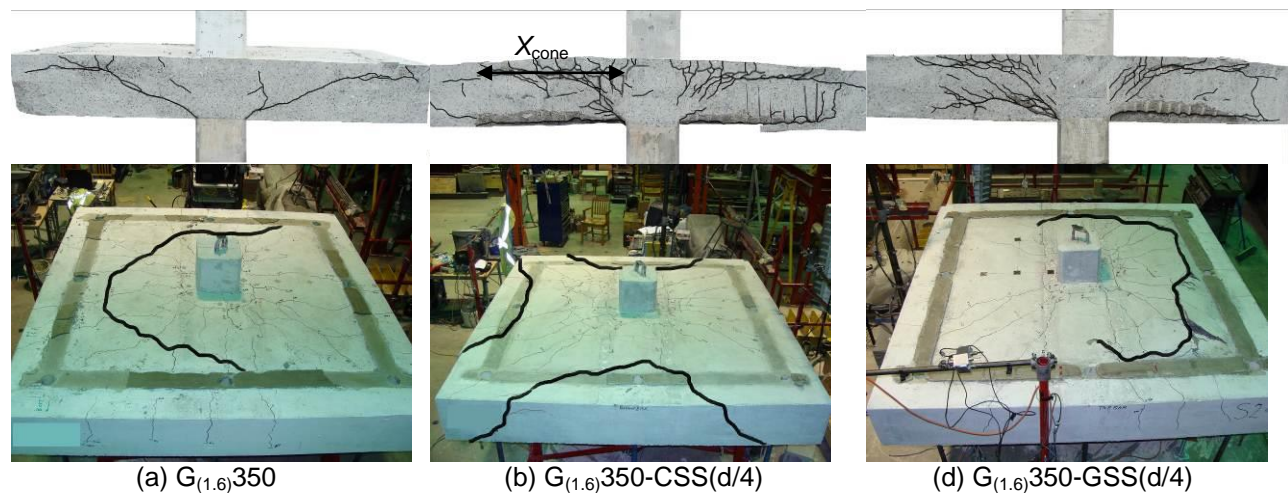


Figure 3: Test specimens at failure

3.3 Shear reinforcement effect

The FRP shear reinforcement plays a significant role in the punching-shear strength and the mode of failure when the percentage of the flexural reinforcement is high enough to ensure punching-shear failure. The test specimens with shear reinforcement transformed the failure into a ductile rather than brittle mode

(Marzouk and Jiang 1997) where the final mode of failure was punching-shear. The presence of the FRP spiral stirrups around the column area affected the slab deformation capacity. In addition, the FRP spiral stirrups confined the flexural reinforcement passing through the column cross-section and led the flexural reinforcement to achieve higher strains.

On the other hand, test specimens with FRP shear reinforcement, exhibited two splitting cracks extended horizontally. The first one appeared in the compression side in the concrete cover. The second one appeared at the level of the tension reinforcement as an extension of the inclined shear cracks. Andersson (1963) tested some specimens with a large amount of shear reinforcement ratios. Through this study it was reported that the radial compressive force in the concrete near the column acts in a nearly horizontal direction. Therefore, a substantial portion of this force is transmitted in the region around and under the lower part of the shear reinforcement. Furthermore, in this region, the radial compressive force changes in direction. Consequently, tensile stresses are produced in a horizontal section through the lower part of the shear reinforcement. In addition, the large amount of shear reinforcement caused an increase in the eccentricity of the radial compressive force in the concrete and therefore also increased the radial tensile stresses at the top surface of the slab. This could explain the development of the two horizontal splitting cracks illustrated in Figure 3 for the specimens with shear reinforcement.

3.4 Flexural reinforcement and concrete strains

Figure 4 shows the load versus reinforcement and concrete strains relationships and Table 4 reports the maximum reinforcement and concrete strains. Figure 4 shows the reinforcement strain values recorded from the electrical strain gauges located at 125 mm from the column centerline and the concrete strain values recorded from the maximum radial concrete gauges close to the column face. The test specimen without shear reinforcement exhibited maximum reinforcement strain of $3199 \mu\epsilon$, which represented 18% of characteristic tensile strength. Besides, the maximum concrete strains near the column region were below the theoretical crushing failure of $3500 \mu\epsilon$ (CSA S806 2012). At failure, however, neither concrete crushing nor rupture of the flexural reinforcement was observed. Thus, the punching-shear capacity of the compression zone was controlled by concrete tension splitting rather than concrete crushing.

Using FRP spiral stirrups (shear reinforcement) in the column zone of the test specimens mobilized the flexural reinforcement to achieve higher strains which led to decompression of the soffit of the slabs. The maximum strains were measured in the $G_{(1.6)350-CSS(d/4)}$ specimen where the concrete strain was $3740 \mu\epsilon$ with no signs of concrete crushing and the reinforcement strain was $6801 \mu\epsilon$.

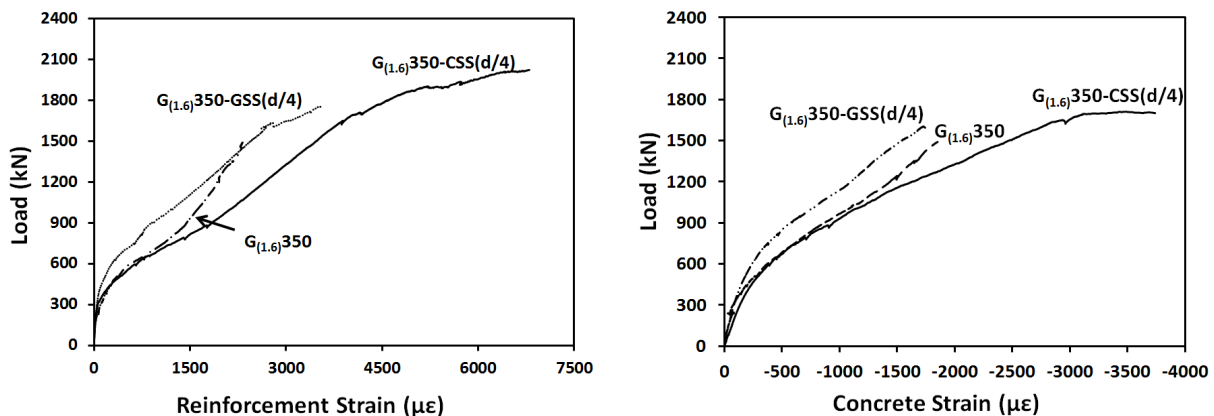


Figure 4: GFRP reinforcement and concrete strains

3.5 FRP stirrups strains

As evidenced from the FRP stirrup strains in Figure 5, the FRP stirrups contribution to the punching-shear resistance before cracking is insignificant. After the development of inclined shear cracks, however, the shear reinforcement transfers most of the forces across the shear cracks and delays further widening. This, in turn, increases the punching-shear capacity of the test specimens. Figure 5 shows the strains in FRP stirrups at $0.5d$ and d from the column face. The strains in FRP stirrups were measured at mid-height of the straight portion of stirrups. It was observed that the GFRP stirrups showed the highest strain values compared to the CFRP stirrups due to the lower modulus of elasticity of GFRP than that of CFRP. Furthermore, there was no rupture in the FRP stirrups at the bend locations.

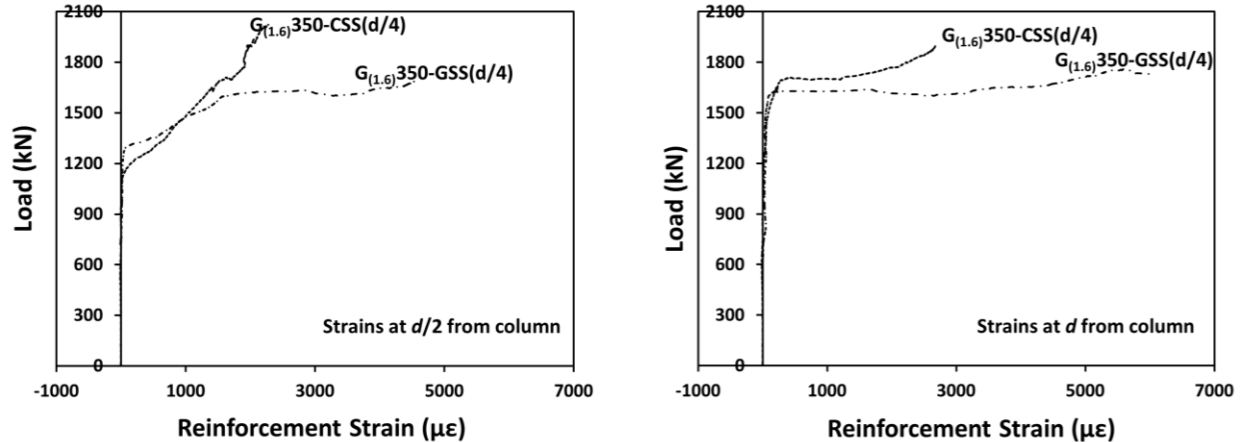


Figure 5: Strains in FRP stirrups located at $d/2$ and d from the column

4 Conclusions

Through this preliminary investigation, three full-scale interior slab-column specimens were constructed and tested under monotonic concentric loading until failure to evaluate the effectiveness of the spiral FRP stirrups in increasing the punching-shear capacity of GFRP-reinforced concrete (GFRP-RC) flat slabs. Based on the experimental results and discussions presented herein, the following conclusions are drawn:

1. FRP spiral stirrups as shear reinforcement play a significant role in enhancing the punching-shear strength of the test specimens. The FRP spiral stirrups increased the punching-shear strength by 16 and 37% for glass and carbon FRP stirrups, respectively.
2. The presences of shear reinforcement in the two-way flat slabs can transform the punching-shear failure into a ductile rather than brittle mode assuming no rupture of stirrups occurs.
3. This preliminary study confirms the efficiency of the FRP spiral stirrups in increasing the punching-shear capacity. More investigations, however, are needed to consider different ratios of flexural and shear reinforcements to clearly understand the behaviour of such members.

5 Acknowledgments

The authors wish to acknowledge the financial support of the Ministère du Développement économique, Innovation et exportation of the province of Quebec. The authors are also grateful to the Pultrall Inc. and the consultant firm EMS Ingénierie inc. for their technical and financial supports. The authors also

acknowledge the support of the Natural Sciences and Engineering Research Council of Canada (NSERC), the Fonds québécois de la recherche sur la nature et les technologies (FQRNT).

6 Notations

The following symbols are used in this paper:

d	= effective slab depth (mm)= (Slab thickness- 45mm- d_b ; where d_b is the bar diameter);
d_b	= the bar diameter (mm);
E_f	= modulus of elasticity of the FRP bars (MPa);
E_{fv}	= modulus of elasticity of the straight portion of FRP stirrups (MPa);
f_c	= cylinders concrete compressive strength (MPa);
f_t	= split cylinder tensile strength of concrete (MPa);
f_{tu}	= ultimate tensile strength of FRP bars;
f_{tu}^*	= characteristic tensile strength FRP bars (MPa);
f_{fv}	= ultimate tensile strength of FRP stirrups straight portion (MPa);
ϵ_{imax}	= maximum tensile strength of FRP bars ($\mu\epsilon$);
ϵ_{cmax}	= ultimate concrete strain ($\mu\epsilon$);
V_{cr}	= first cracking load (kN);
V_u	= ultimate punching shear load (measured in test) (kN);
v_u	= ultimate shear stress at $0.5d$ from the column face (MPa);
$b_{o,0.5d}$	= critical perimeter at a distance of $0.5d$ from the column face (mm);
X_{cone}	= distance from the column face to the observed failure surface;
ρ_f	= FRP reinforcement ratio;
ρ_{fv}	= shear reinforcement ratio at a perimeter at $0.5d = (n_s \cdot A_{fv} / S_{fv} \cdot b_{o,0.5d})$.
$\rho_{fv} E_f$	= shear reinforcement index.

7 References

- Andersson, J. 1963. Punching of Concrete Slabs with Shear Reinforcement. Transactions 212, *Royal Institute of Technology*, Stockholm.
- ASTM D7205. 2011. Tensile Properties of Fiber Reinforced Polymer Matrix Composite Bars. *American Society for Testing and Materials*, Conshohocken, USA, 12 p.
- Benmokrane, B., Ahmed, E., Dulude, C., Boucher, E. 2012. Design, Construction, and Monitoring of the First Worldwide Two-Way Flat Slab Parking Garage Reinforced with GFRP Bars. *Proceedings of the 6th International Conference on FRP Composites in Civil Engineering*, Rome, Italy, June 13-15, 8 p.
- Canadian Standards Association (CSA). 2010. *Specification for Fibre-Reinforced Polymers. (CAN/CSA S807-10)*, Rexdale, Ontario, Canada, 27 p.
- Canadian Standards Association (CSA). 2012. *Design and Construction of Building Structures with Fibre Reinforced Polymers. (CAN/CSA S806-12)*, Rexdale, Ontario, Canada, 198 p.
- El-Ghandour, A.W., Pilakoutas, K., Waldron, P. 2003. Punching Shear Behavior of Fiber Reinforced Polymers Reinforced Concrete Flat Slabs: Experimental Study. *ASCE Journal of Composites for Construction*, 7(3): 258–265.
- Marzouk, H. and Jiang, D. 1997. Experimental Investigation on Shear Enhancement Types for High-Strength Concrete Plates. *ACI Structural Journal*, 94 (1): 49-58.
- Zaghloul, A. 2007. Punching Shear Strength of Interior and Edge Column-Slab Connections in CFRP Reinforced Flat Plate Structures Transferring Shear and Moment. *PhD thesis*, Department of Civil and Environmental Engineering, Carleton University, Ottawa, Ontario.